2009-01-01

Effect of Organic Chelates on the Performance of Hybrid Sol–Gel Coated AA2024-T3 Aluminium Alloys

Rajath Varma
Technological University Dublin, rajath.varma@tudublin.ie

John Colreavy
Technological University Dublin, john.colreavy@tudublin.ie

John Cassidy
Technological University Dublin, john.cassidy@tudublin.ie

See next page for additional authors

Recommended Citation

Varma, R. et al. (2009) :Effect of Organic Chelates on the Performance of Hybrid Sol–Gel Coated AA2024-T3 Aluminium Alloys. *Progress in Organic Coatings*, Volume 66, Issue 4, December 2009, pp.406-411. doi:10.1016/j.porgcoat.2009.09.004

Funder: Enterprise Ireland

Progress in Organic Coatings xxx (2009) xxx–xxx

Contents lists available at ScienceDirect

Progress in Organic Coatings

journal homepage: www.elsevier.com/locate/porgcoat

Effect of organic chelates on the performance of hybrid sol–gel coated AA 2024-T3 aluminium alloys

P.C. Rajath Varma[a], John Colreavy[a], John Cassidy[b], Mohamed Oubaha[c], Brendan Duffy[a,*], Collette McDonagh[c]

[a] Centre for Research in Engineering Surface Technology (CREST), FOCAS Institute, Dublin Institute of Technology, 13 Camden Row, Dublin 8, Ireland
[b] School of Chemical and Pharmaceutical Sciences, Dublin Institute of Technology, Kevin St., Dublin 8, Ireland
[c] National Centre for Sensor Research (NCSR), Dublin City University, Dublin 9, Ireland

ARTICLE INFO

Article history:
Received 12 September 2008
Received in revised form 12 August 2009
Accepted 4 September 2009

Keywords:
Ormosil
Zirconium
Chelate
Coating
Nanoparticles

ABSTRACT

Sol–gels are organic–inorganic polymers formed by hydrolysis/condensation reactions of alkoxide precursors, primarily silanes, which have found applications as electronic, optical and protective coatings. These coatings possess important characteristics such as chemical stability, physical strength and scratch resistance. Further performance improvement is achieved through the incorporation of zirconium and titanium based nanoparticles, also formed through the sol–gel process. However due to the inherent difference in the reactivity of the precursors, the hydrolysis of each precursor must be carried out separately before being combined for final condensation. Zirconium precursors are commonly chelated using acetic acids, prior to hydrolysis, to lower the hydrolysis rate.

In this body of work various ligands such as organic acids, acetyl acetone (AcAc) and 2,2′-bipyridine (Bipy) were used to control the zirconium hydrolysis reaction and form nanoparticles within the silane sol matrix.

Nanoparticle modified coatings formed from the silane sol on AA 2024-T3 aluminium were characterised spectroscopically, electrochemically and calorimetrically to evaluate the potential effect of the different chelates on the final film properties while neutral salt spray tests were performed to study their anti-corrosion performance. Results indicate that the acid ligand modified coatings provided the best performance followed by AcAc, while Bipy was the poorest. In all cases the zirconium nanoparticle improved the protective properties of the sol–gel coating.

1. Introduction

As the most abundant metal in the Earth's crust (8.1%), aluminium is used extensively in alloys for products ranging from kitchen utensils and drink cans to engineering, architectural and automotive applications. However aluminium is not found free in nature, but chiefly as bauxite due to its reactivity. Consequently products with high aluminium content need to be protected from atmospheric conditions in order to maintain their appearance and performance. This is important if the alloy contains high levels of secondary phase particles, such as copper intermetallics, which may promote galvanic activity. Until recently the current state of art for protecting aluminium alloys involved the use of hexavalent chromium technology [1]. However in the interest of human health [2,3] and environmental concerns, alternative solutions are being pursued. For engineering applications organic polymers (polyesters, polyamides, alkyds, polyurethane) [4], conductive polymers (polyaniline and polypyrrole) [4,5] and sol–gel derived organic–inorganic hybrid materials have emerged as a promising Cr^{6+} alternatives [6].

The sol–gel process can be used to form nanostructured inorganic films (typically 200 nm to 10 μm in overall thickness) that are more resistant than metals to oxidation, corrosion, erosion and wear while also possessing good thermal and electrical properties. The chemistry of the sol–gel process is well known [7–9] with excellent reviews [6,10,11] and books [12] available. The most common sol–gel materials used as coatings are based on organically modified silicates (ormosils), which are formed by the hydrolysis and condensation of organically modified silanes with alkoxide precursors [13,14].

Initial studies of ormosils as protective coatings on aluminium [15,16] found that they lacked chromium's self-healing properties. However the combination of ormosils and zirconium chemistries were found to improve the coatings performance considerably [17], especially alkali resistance. Some United States Air Force studies investigated several routes towards improving performance including the use of rare-earth metal salts [18], amine cross-linkers [19–21], supramolecular inclusion and organic inhibitors [22,23].

* Corresponding author. Tel.: +353 1 402 7964; fax: +353 1 402 7941.
E-mail address: bduffy@dit.ie (B. Duffy).

0300-9440/$ – see front matter © 2009 Elsevier B.V. All rights reserved.
doi:10.1016/j.porgcoat.2009.09.004

Similar approaches were investigated by Ferreira's group in Portugal which concentrated on epoxy functionalised silane–zirconium systems by adding cerium [24], azole based organic inhibitors in host molecules [25,26] and bis-silanes [27]. This group has also published data which suggests the route of zirconium inclusion is important, as the choice of chelating ligand may have an effect of the final coating performance [28]. This would be in agreement with the previous studies which found that hydrolysis of zirconium alkoxides can be controlled to deliver nanoparticles of varying sizes [29,30].

The aim of this work is to study the performance of hybrid sol–gel coatings on AA 2024-T3 aluminium alloy while varying the ligands used to chelate the zirconium precursor. Zirconium n-propoxide was chelated with three carboxylic acids (methacrylic, acetic and isobutyric acid), a β-diketone (AcAc) and Bipy to form nanoparticles within a silane matrix based on 3-(trimethoxysilyl)propylmethacrylate (MAPTMS). Once applied as a coating, the influence of the ligand on the physical properties was studied using Fourier transform infra-red (FTIR) spectroscopy, differential scanning calorimetry (DSC) and dynamic light scattering (DLS). The electrochemical behaviour of the coatings was studied using potentiodynamic scanning (PDS) and electrochemical impedance spectroscopy (EIS). Long term performance was evaluated using neutral salt spray test.

The results indicate that the effect of ligands on performance of hybrid coatings is very significant, especially in harsh environments where aluminium alloys are dependant on protective coatings for long term usage.

2. Experimental

2.1. Synthesis of hybrid sols

The sols were prepared according to the experimental schematic in Fig. 1. The silane precursor, 3-(trimethoxysilyl) propylmethacrylate (MAPTMS) (Sigma–Aldrich, Ireland, assay ~99%) was pre-hydrolysed using 0.01N HNO_3 for 45 min (A). Simultaneously, zirconium (IV) n-propoxide (TPOZ) (Sigma–Aldrich, Ireland, assay ~70% in propanol) was chelated using one of five ligands (Table 1), at a 1:1 molar ratio for 45 min (B) to form a zirconium complex. All of the ligands (acetic acid, isobutyric acid, methacrylic acid, acetylacetone and 2,2′-bipyridine) were purchased from Sigma–Aldrich (Ireland) and used without further modification. Solution A was slowly added to solution B over 10 min. The mixture of A with B is characterised by an exothermic reaction indicating the hydrolysis of the remaining propoxy bonds on the zirconium precursor, rather than a physical dispersion, was occurring. Following another 45 min, water (pH 7) was added to this mixture to give a final molar ratio of 2.5:1:1:5 (MAPTMS:ligand:TPOZ:H_2O), as used previously [31]. For description purposes the final sol–gel coating materials will be referred in shorthand notation as Si/Zr/ligand (e.g. Si/Zr/AcOH).

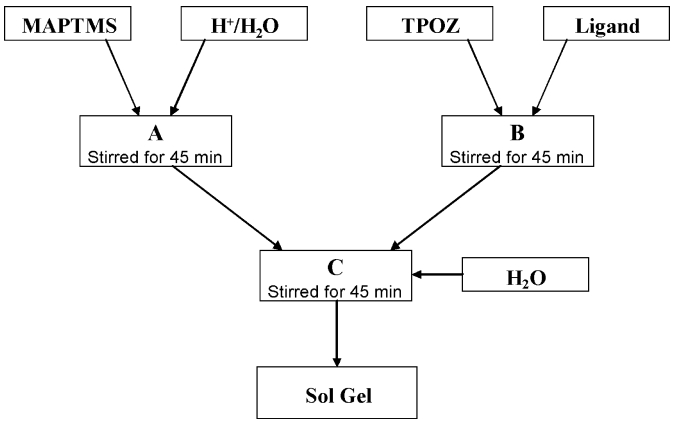

Fig. 1. Flow chart for the preparation of hybrid sols.

Table 1
Ligand used to chelate TPOZ.

Ligand		
Name	Abbreviation	Structure
Acetic acid	AcOH	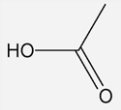
Isobutyric acid	IBA	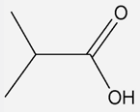
Methacrylic acid	MAAH	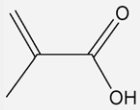
Acetylacetone	AcAc	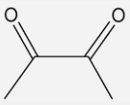
2,2′-Bipyridine	Bipy	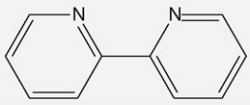

2.2. Preparation of sol–gel coating

AA2024-T3 aluminium panels (150 mm × 100 mm) were sourced from Amari Irl, Clondalkin. The panels were degreased with isopropanol, alkaline cleaned using Oakite 61 B® (Chemetall, UK) by immersion at 60 °C for 1 min and washed in warm deionised water. Any smut was removed by washing in 10% nitric acid (Sigma, Ireland) and washed in deionised water. The sols were filtered using a 0.45 μm syringe filter and applied by spin coating on AA 2024-T3 alloy at up to 1000 rpm and cured for 12 h at 100 °C. The final thickness of all sol–gel coating was 3.5 μm (±0.5 μm), as measured using an Isoscope® non-destructive coating thickness gauge. All finishes were touch dry within 24 h, with a gloss finish.

2.3. Measurements

The electrochemical data was obtained using a Solartron SI 1287/1255B system comprising of frequency analyser and potentiostat. Potentiodynamic scanning was performed using an electrochemical cell (PAR K0235 Flat Cell) with an exposed area of 0.78 cm^2 in a continually aerated Harrison's solution (3.5 wt.% $(NH_4)_2SO_4$ and 0.5 wt.% NaCl) where the coated metal acted as a working electrode, a silver/silver chloride (Ag/AgCl) electrode was used as a reference electrode and platinum mesh as a counter electrode. All scans were acquired in the region from −0.4 to +0.5 V vs. E_{oc}, with a scan rate 20 mV/s at room temperatures (20 ± 2 °C).

Please cite this article in press as: P.C.R. Varma, et al., Effect of organic chelates on the performance of hybrid sol–gel coated AA 2024-T3 aluminium alloys, Prog. Org. Coat. (2009), doi:10.1016/j.porgcoat.2009.09.004

Electrochemical impedance data was performed using the electrochemical cells prepared by slicing polypropylene sample bottles (2.5 cm diameter) 10 mm from the base which were then secured on the sol–gel coated aluminium substrate using a 2 K epoxy adhesive (Araldite, Radionics (Ireland)). A dilute Harrison's solution was used as electrolyte (0.35 wt.% $(NH_4)_2SO_4$ and 0.05 wt.% NaCl). All measurements were made at the open circuit potential (OCP, E_{oc}) with an applied 10 mV sinusoidal perturbation in the frequency range 1×10^6 to 1×10^{-2} Hz (10 points per decade).

Samples for differential scanning calorimetry (DSC) were prepared by dropping 10 μl of the sol into aluminium sample pans and curing at 100 °C for 1 h in an oven. DSC measurements were carried out using a Rheometric Scientific DSC QC instrument under an air atmosphere at a heating rate of 10 °C/min between 50 and 400 °C.

Sol–gel particle sizes were determined using a Malvern Nano-ZS instrument, using the Dynamic light scattering (DLS) technique.

The chemical bonding within the zirconium complexes was characterised by Fourier Transform Infrared Spectroscopy (FTIR, PerkinElmer GX). The solution B was dried at 100 °C for 12 h. The dried powders were then crushed with KBr pellets to form disks and analysed in transmission mode.

The corrosion resistance of the coated AA2024-T3 alloys was evaluated by exposure of the scribed samples to salt fog atmosphere generated from 5 wt.% aqueous NaCl solution at 35 (±1) °C for 168 h according to ASTM B117 specifications. The edges and backs of all panels were protected using a two pack epoxy coating prepared using Desmophen A365 and Desmodure N75 (Bayer AG, Germany). The sides were also taped using insulating tape.

3. Results and discussion

3.1. FTIR results

FTIR spectroscopy is a powerful characterisation technique to identify the coordination mode of a carboxylate ligand in metal carboxylates [29]. To identify the effect of the ligands on the nature of the coordination with the zirconium atom, 5 complexes were synthesised and respective infrared spectra recorded in the 1300–1800 cm^{-1} spectral range, as represented in Table 2. This is well known to be the region where the carboxylic vibration bands are usually identified [32]. Within this spectral window TPOZ shows 6 absorption bands centred at 1350, 1360, 1380, 1440, 1460 and 1470 cm^{-1} ascribable to the stretching vibrations of the aliphatic CH groups contained in the propoxide group [33]. The absorption vibrations involving the Zr–OPr group are primarily located in the range 800–1300 cm^{-1} [34] and do not show any absorption beyond 1500 cm^{-1}. Within the 1300–1800 cm^{-1} spectral range, the chelated TPOZ shows several absorption bands inherent to the fundamental vibration of the zirconium nanoparticle [31].

Table 2
FTIR peak assignation for chelated zirconium precursors in the 1300–1800 cm^{-1} region.

Ligand	Wavenumber (cm^{-1})	Inference
AcOH	1548	υ_{as} COO^-
	1446	υ_s COO^-
IBA	1542	υ_{as} COO^-
	1477	υ_s COO^-
	1430	δ CH_3
MAAH	1770	C=O
	1550	υ_{as} COO^-
	1448	υ_s COO^-
AcAc	1598	γ C=O (bonded AcAc—enol form)
	1523	υ C=C (bonded AcAc—enol form)
	1373	δ Zr–O
Bipy	1565	Zr–N
	1315	C–N

Scheme 1. Keto-enolic equilibrium of the acetylacetone molecule.

The Zr/ligand complexes synthesised with carboxylic acids ligands (MAAH, IBA, and AcOH) have two peaks in the 1500–1700 cm^{-1} region, which are clearly ascribable to the symmetric (ν_s) and asymmetric stretching (ν_{as}) vibrations of the carboxylic group (COO^-) respectively [35]. With typical $\Delta\upsilon(COO^-)$ of between 75 and 125 cm^{-1}, all complexes can be said to act as bidentate chelates.

Two bands are observed at 1598 and 1523 cm^{-1} for the Zr/ligand complexes synthesised with AcAc that can be attributed to the formation of the carbonyl and vinyl bonds within the prevalent keto-enol form of the ketone (Scheme 1).

In this configuration the unsaturated vinylic group acts as an auxochromic group, then provoking a bathochromic shift of the carbonyl group via a mesomeric effect. It is possible that the complex synthesised with AcAc can exist in two different configurations, due to the presence of the methylene bridge in the aliphatic chain between the ketone and the alcohol functions, which can confer a higher flexibility to the molecule facilitating binding with two different zirconium atoms, thereby increasing the size of the particles.

The complex synthesised with Bipy as chelating agent shows the disappearance of the main absorption bands associated to the Bipy absorption (1414, 1451, 1457, and 1578 cm^{-1}) and the appearance of a broad band (measuring about 320 cm^{-1}) centred at 1565 cm^{-1}. Basically, Bipy can only react with TPOZ by coordination bonds involving the nitrogen atom and the free d orbitals of the zirconium atom. Similarly to AcAc, Bipy is potentially bidentate and can potentially react with two different zirconium atoms in its trans form, potentially forming oligomers of different sizes. However, by both the electronic attraction (mesomeric effect) and sterical hindrance of the aromatic structure, Bipy can provoke distortions of the spatial configuration of the oligomers formed. Both phenomena can contribute to the molecular dispersion, the result of which is observed as the broadening of the fundamental absorption of the metal-ligand vibration.

From the analysis of the IR spectra, two conclusions can be drawn. Firstly the formation of zirconium complexes with organic ligands is clearly evidenced in this work. Secondly, the nature of the organic ligand has an effect on the size of the zirconium particles. Indeed, it seems that the carboxylic acids tend to form complexes with only one zirconium atom, whereas AcAc and Bipy have the ability to form oligomers with different degrees of condensation.

3.2. Thermal stability

DSC analysis was performed on cured sol–gel materials between 25 and 400 °C, although the working temperature for a typical coating would be likely to be below 250 °C. The results indicate that the ligand choice has a profound effect on the glass transition temperature (T_g) of each material (Table 3). Two distinct transitions can be attributed to the zirconium nanoparticles and the silane network. It was found that the zirconium nanoparticles formed using MAAH and AcOH display higher T_g, while Bipy is lowest. This highlights the difference (by up to 80 °C) in the chelating ability of the ligand and is related to the metal-ligand charge transfer stability. There is less variation in the T_g for the silane network which remains consistent in the 300–320 °C region. Therefore it is reasonable to infer

Please cite this article in press as: P.C.R. Varma, et al., Effect of organic chelates on the performance of hybrid sol–gel coated AA 2024-T3 aluminium alloys, Prog. Org. Coat. (2009), doi:10.1016/j.porgcoat.2009.09.004

Table 3
Physical data for ormosil coatings.

Zirconium chelate	T_g	Particle sizes (nm)
No zirconium	130	2.3[a]
AcOH	260, 310	0.83[b], 7.5[a]
IBA	240, 320	1.5[b], 8.7[a]
MAAH	260, 305	0.96[b], 2.6[a]
AcAc	205, 250	1.17[b], 6.5[a]
Bipy	180, 320	2[b], 8.7[a], 122[c]

[a] Silane sol.
[b] Zirconium chelated nanoparticle.
[c] Bipy oligomer.

that the thermal stability of the acid chelated complexes is superior to the weaker basic bonded ligands.

3.3. Particle size analysis

Particle size measurements (Table 3) indicate the level of influence the ligands have on the formation of the Zirconium nanoparticles. The lowest particle sizes are Si/Zr/AcOH and Si/Zr/MAAH, followed by Si/Zr/AcAc, Si/Zr/IBA and finally Si/Zr/Bipy. Interestingly Si/Zr/Bipy seems to have formed particles in the 120 nm range, potentially oligomers as discussed previously.

3.4. Electrochemical testing

The electrochemical properties of the sol–gel coatings give vital early information on the potential long term performance in aggressive challenging environments. Potentiodynamic scanning (PDS) is a DC technique that gives useful information on a coatings ability to resist corrosion against a voltage gradient, while electrochemical impedance spectroscopy (EIS) is an AC technique is used to estimate electrochemical interactions at the coating metal interface at a preset potential, usually the open circuit potential.

3.4.1. PDS

Using Harrison's solution potentiodynamic evaluation involves applying a voltage from 0.5 V below the open circuit potential (cathodic region) to 0.4 V above it (anodic region). Therefore the degree of change in the current density (electrons exchange occurring at the electrodes) is a function of the potential applied. If a high enough potential (overpotential) is applied then corrosion is accelerated. Therefore a coating that maintains a low current density at high overpotential is desirable. The coating properties such as corrosion current densities (I_{corr}) and potential (E_{corr}) were estimated by the Tafel method [36], while the polarisation resistance (R_p) was calculated using Stern–Geary equation [37] (Eq. (1)).

$$I_{corr} = \frac{B}{R_p} \quad (1)$$

where R_p is the polarisation resistance and B is a proportionality constant for the particular system which is calculated from and the slopes of the anodic (β_a) and cathodic (β_c) Tafel regions as shown by Eq. (2).

$$B = \frac{\beta_a \cdot \beta_c}{2.3(\beta_a + \beta_c)} \quad (2)$$

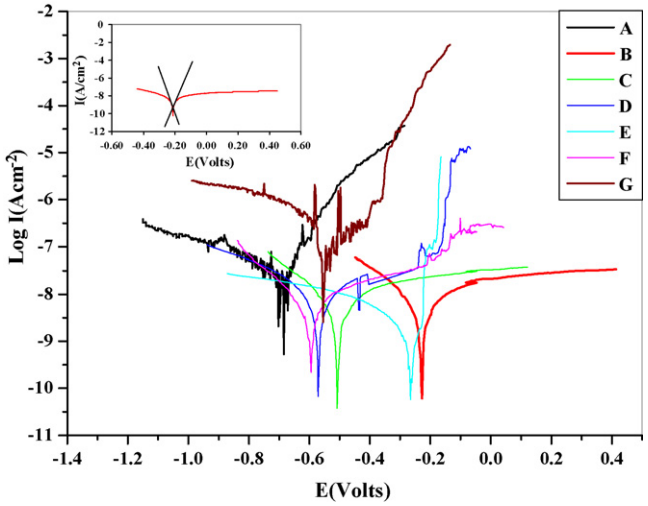

Fig. 2. Potentiodynamic scan plots for various sol–gel coatings: (A) MAPTMS and Si/Zr modified with various ligands such as (B) MAAH, (C) AcOH, (D) IBA, (E) AcAc, (F) BP, (G) Bare AA2024 (inset: extrapolation of data in Tafel region of (B)).

I_{corr}, E_{corr} and the Tafel coefficients for all coatings are listed in Table 4. It should be noted that as the solution was agitated by aeration and not stirring, and considering that the metallic surface is covered by a coating, the rate determining step of the electrode process is probably not the activation of that charge transfer and thus, the physical values in Table 4 can only be used to differentiate the samples qualitatively, but not quantitatively.

The use of an organosilane reduced the apparent corrosion current density by an order in magnitude versus bare AA2024-T3. The improvement can be attributed to the adhesion of a nanostructured silane coating to the alloy surface. With little change in the E_{corr} value it is clear that the coating does not inhibit any electrochemical activity on the surface, but retards the ingress of water and/or oxygen. Further improvement in the performance of the organosilane was achieved by the introduction of the zirconium nanoparticles. The beneficial impact of the nanoparticles is observed when comparing the apparent coating resistances (R_p). The methacrylic and acetic acids providing the best improvements (no E_{Pit} observed) while the basic nitrogen bonding Bipy provided the least. The hierarchy of performance is in broad agreement with the thermal stability data and confirms that importance of the ligand on the nanoparticle formation (Fig. 2).

3.4.2. EIS

EIS involved applying an AC voltage at the OCP, with sinusoidal amplitude of 10 mV, from a frequency of 10^6 Hz down to 10^{-2} Hz across a coating in contact with Dilute Harrison's solution. The coat-

Table 4
Electrochemical data for sol–gel coatings.

Substrate coating	I_{corr} (A cm^{-2})	E_{corr} (V)	R_p (Ω cm^2)	$\lvert\beta_a\rvert$ (V/decade)	$\lvert\beta_c\rvert$ (V/decade)	E_{Pit} (V)
None (bare AA 2024-T3)	8.15×10^{-8}	−0.525	2.05×10^6	0.0943	0.125	
MAPTMS (Si)	6.87×10^{-9}	−0.662	1.32×10^7	0.0689	0.103	−0.6
Si/Zr/AcOH	1.41×10^{-9}	−0.472	5.50×10^7	0.0553	0.080	–
Si/Zr/IBA	2.05×10^{-9}	−0.560	2.93×10^7	0.0542	0.089	−0.15
Si/Zr/MAAH	1.39×10^{-9}	−0.148	6.50×10^7	0.0552	0.075	–
Si/Zr/AcAc	2.57×10^{-10}	−0.254	3.20×10^7	0.0148	0.067	−0.21
Si/Zr/Bipy	1.15×10^{-9}	−0.564	1.64×10^7	0.0265	0.068	−0.17

Please cite this article in press as: P.C.R. Varma, et al., Effect of organic chelates on the performance of hybrid sol–gel coated AA 2024-T3 aluminium alloys, Prog. Org. Coat. (2009), doi:10.1016/j.porgcoat.2009.09.004

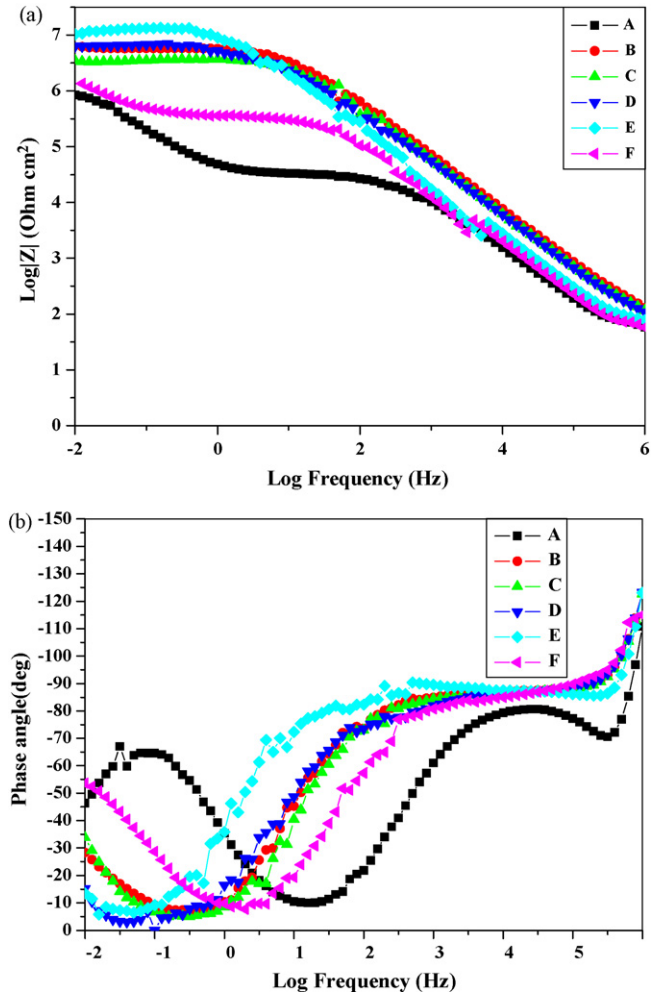

Fig. 3. Bode plots of coatings after 1 h immersion in dilute Harrison's solution (A) MAPTMS and Si/Zr modified with various ligands such as (B) MAAH, (C) AcOH, (D) IBA, (E) AcAc, (F) Bipy.

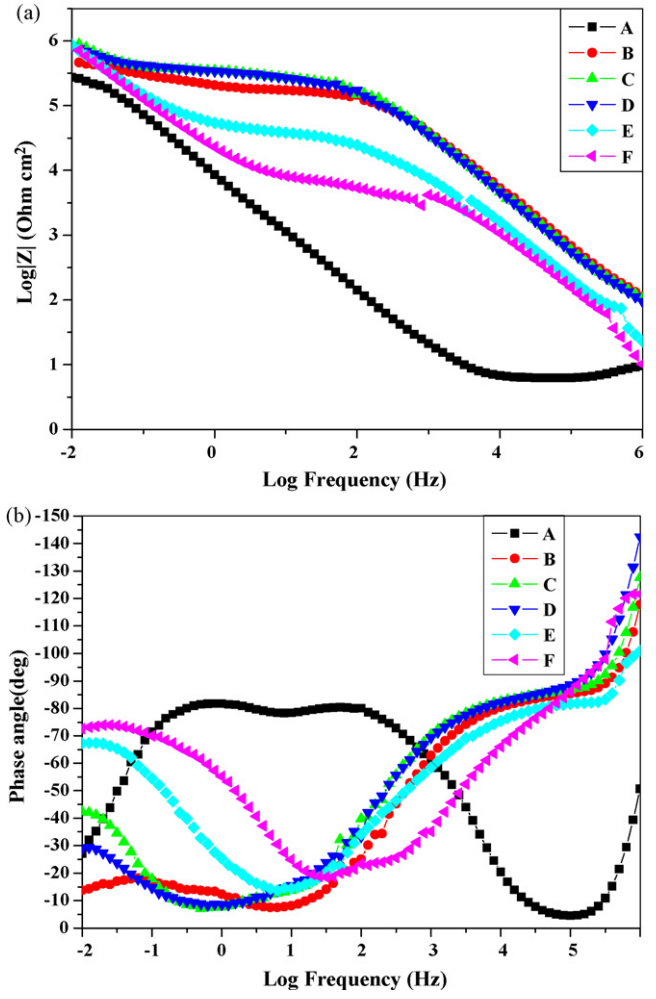

Fig. 4. Bode plots of coatings after 72 h immersion in dilute Harrison's solution (A) MAPTMS and Si/Zr modified with various ligands such as (B) MAAH, (C) AcOH, (D) IBA, (E) AcAc, (F) Bipy.

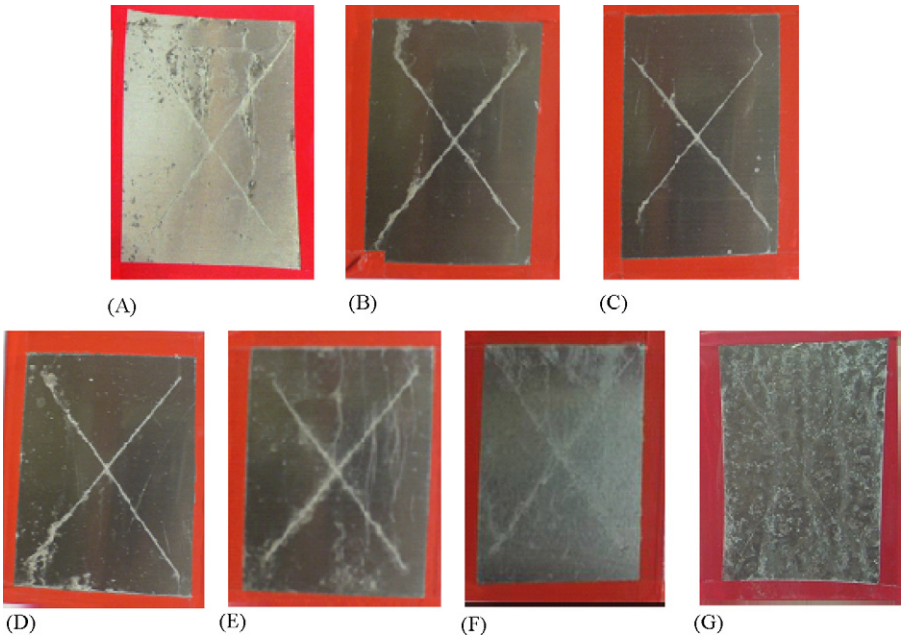

Fig. 5. Salt spray results plots for various sol–gel coatings: (A) MAPTMS for 48 h and Si/Zr modified with various ligands such as (B) MAAH, (C) AcOH, (D) IBA, (E) AcAc, (F) BP for 1 week, (G) Bare AA2024 after 24 h.

Please cite this article in press as: P.C.R. Varma, et al., Effect of organic chelates on the performance of hybrid sol–gel coated AA 2024-T3 aluminium alloys, Prog. Org. Coat. (2009), doi:10.1016/j.porgcoat.2009.09.004

ings resistance to the AC signal, or impedance, varies according to the applied frequency and is graphically represented on a Bode frequency plot. The phase angle associated with the impedance gives valuable information on the film properties such as barrier performance and interfacial activity. This activity is often seen as a build up of oxide material, which may prevent charge transfer at the metal surface thus increasing the effective interface capacitance. The technique can be modelled as an equivalent electrical circuit as explained elsewhere [38].

The impedance data for the hybrid coatings is shown after initial electrolyte (Dilute Harrison's solution) exposure (Fig. 3(a and b)) and 72 h exposure (Fig. 4(a and b)). The most apparent drop in impedance performance is seen with MAPTMS alone, which can be interpreted as electrolyte ingress and interface corrosion (φ increased to -80° at 10^{-1} Hz). In contrast Si/Zr/MAAH performs best, maintaining high impedance with a minimal phase lag (φ remaining below -20° at 10^{-2} Hz). As with the DSC study, the acid chelated systems appear to be the most stable and resistant to corrosion product formation.

3.5. Neutral salt spray test

Neutral salt spray test were conducted for 1 week under ASTM B117 conditions. The first panels to fail were coated with MAPTMS alone, after 48 h (Fig. 5). The hybrid coatings performed better and all panels were exposed for 1 week. The coatings based on Si/Zr/MAAH and Si/Zr/AcOH performed best, corroding only along the scribe with little pitting observed. The same order of performance as seen with DSC, EIS and PDS was observed, whereby Si/Zr/IBA coating outperformed the AcAc and Si/Zr/Bipy chelated equivalents. Pitting was observed for the Si/Zr/IBA coating, to a greater extent on the Si/Zr/AcAc coating with extensive corrosion product present on the Si/Zr/Bipy film. The presence of pitting indicates that the copper intermetallics at the alloy surface are not being passivated, which confirms the PDS data where E_{Pit} values in the -0.1 to -0.2 V were observed.

4. Conclusion

Various ligands were used to form Zirconium nanoparticles within an ormosil coating on AA2024-T3 aluminium, to improve its performance under aggressive conditions. The electrochemical studies and neutral salt spray results indicated that the zirconium nanoparticles significantly improved the performance of the ormosil coating, with nanoparticles formed using carboxylic acid offering the best protection. The improved performance of the acid modified ligands can be attributed to the formation of much smaller size particles of ZrO_2 during the hydrolysis and condensation process thus providing a greater degree of thermal stability to the polymer network. The use of other ligand such as AcAc and Bipy may have resulted in formation of the larger size particles, and thus a less compact polymer network which allowed the ingress of electrolyte to promote corrosion.

Acknowledgement

The authors would like to thank Enterprise Ireland for financial support, through the Dualion Project (CFTD/05/306).

References

[1] J. Zhao, L. Xia, A. Sehgal, D. Lu, R.L. McCreery, G.S. Frankel, Surf. Coat. Technol. 140 (2001) 51–57.
[2] T.L. Metroke, J.S. Gandhi, A. Apblett, Prog. Org. Coat. 50 (2004) 23.
[3] N.N. Voevodin, N.T. Grebasch, W.S. Soto, F.E. Arnold, M.S. Donley, Surf. Coat. Technol. 140 (2001) 16.
[4] R.L. Twite, G.P. Bierwagen, Prog. Org. Coat. 33 (1998) 91.
[5] I. Jerman, A.S. Vuk, M. Kozelj, B. Orel, J. Kovec, Langmuir 24 (2008) 5029–5037.
[6] M.L. Zheludkevich, I. Miranda Salvado, M.G.S. Ferreira, J. Mater. Chem. 15 (2005) 5099–5111.
[7] J. Livage, M. Henry, C. Sanchez, Prog. Solid State Chem. 288 (1988) 259.
[8] C.J. Brinker, G. Scherrer, Sol–Gel Science: The Physics and Chemistry of Sol–Gel Processing, Academic Press, San Diego, CA, 1990.
[9] L.L. Hench, J.K. West, Chem. Rev 90 (1990) 33.
[10] M. Guglielmi, J. Sol–Gel Sci. Technol. 8 (1997) 443–449.
[11] C. Sanchez, B. Julian, P. Belleville, M. Popall, J. Mater. Chem. 15 (2005) 3559–3592.
[12] C. Sanchez, P. Gomez-Romero, Functional Hybrid Materials, Wiley VCH, Weinheim, ISBN-13-978-3-527-30484-4, 2004.
[13] R.L. Parkhill, E.T. Knobbe, M.S. Donley, Prog. Org. Coat. 41 (2001) 261.
[14] R. Kasemann, H. Schmidt, First European Workshop on Hybrid Organic–Inorganic Materials, Chateau de Bierville, France, 1993, 8–10 November, p. 171.
[15] M. Khobaib, L.B. Reynolds, M.S. Donley, Surf. Coat. Technol. 140 (2001) 16–23.
[16] N. Voevodin, C. Jeffcoate, L. Simon, M. Khobaib, M.S. Donley, Surf. Coat. Technol. 140 (2001) 29–34.
[17] N.N. Voevodin, N.T. Grebasch, W.S. Soto, L.S. Kasten, J.T. Grant, F.E. Arnold, M.S. Donley, Prog. Org. Coat. 41 (2001) 287–293.
[18] N.N. Voevodin, N.T. Grebasch, W.S. Soto, F.E. Arnold, M.S. Donley, Surf. Coat. Technol. 140 (2001) 24–28.
[19] M.S. Donley, R.A. Mantz, A.N. Khramov, V.N. Balbyshev, L.S. Kasten, D.J. Gaspar, Prog. Org. Coat. 47 (2003) 401–415.
[20] L.S. Kasten, V.N. Balbyshev, M.S. Donley, Prog. Org. Coat. 47 (2003) 214–224.
[21] A.N. Khramov, V.N. Balbyshev, N.N. Voevodin, M.S. Donley, Prog. Org. Coat. 47 (2003) 401–415.
[22] A.N. Khramov, N.N. Voevodin, V.N. Balbyshev, M.S. Donley, Thin Solid Films 447 (2004) 549–557.
[23] A.N. Khramov, N.N. Voevodin, V.N. Balbyshev, R.A. Mantz, Thin Solid Films 483 (2005) 191–196.
[24] M.L. Zheludkevich, R. Serra, M.F. Montemor, M.G.S. Ferreira, Electrochem. Commun. 7 (2005) 836–840.
[25] M.L. Zheludkevich, K.A. Yasakau, S.K. Poznyak, M.G.S. Ferreira, Corros. Sci. 47 (2005) 3368–3383 (b).
[26] D.G. Shchukin, M. Zheludkevich, K. Yasakau, S. Lamaka, M.G.S. Ferreira, H. Mohwald, Adv. Mater. 18 (2006) 1672–1678.
[27] M.F. Montemor, W. Trabelsi, M. Zheludevich, M.G.S. Ferreira, Prog. Org. Coat. 57 (2006) 67–77.
[28] S.K. Poznyak, M.L. Zheludkevich, D. Raps, F. Gammel, K.A. Yasakau, M.G.S. Ferreira, Prog. Org. Coat. 62 (2008) 226–235.
[29] M. Chatry, M. Henry, M. In, C. Sanchez, J. Livage, J. Sol–Gel Sci. Technol. 1 (1994) 233–240.
[30] H. Hayashi, H. Suzuki, S. Kaneko, J. Sol–Gel Sci. Technol. 12 (1998) 87–94.
[31] M. Oubaha, P. Etienne, S. Calas, R. Sempere, J.M. Nedelec, Y. Moreau, J. Non-Cryst. Solids 351 (2005) 2122–2128.
[32] F.X. Perrin, V. Nguyen, J.L. Vernet, J. Sol–Gel Technol. 28 (2003) 205.
[33] D. Hoebbel, T. Reinert, H. Schmidt, J. Sol–Gel. Sci. Technol. 10 (1997) 115–126.
[34] F. Rubio, J. Rubio, J.L. Oteo, J. Mater. Sci. Lett. 17 (1998) 1839–1842.
[35] Z. Weihua, Z. Gaoyang, C. Zhiming, Mater. Sci. Eng. B 99 (2003) 168–172.
[36] M. Kendig, S. Jeanjaquet, R. Addison, J. Waldrop, Surf. Coat. Technol. 140 (2001) 58–66.
[37] V. Barranco, S. Feliu Jr., S. Feliu, Corr. Sci. 46 (2004) 2203–2220.
[38] M.L. Zheludkevich, R. Serra, M.F. Montemor, K.A. Yasakau, I.M. Miranda Salvado, M.G.S. Ferreira, Electrochim. Acta 51 (2005) 208–217.

Please cite this article in press as: P.C.R. Varma, et al., Effect of organic chelates on the performance of hybrid sol–gel coated AA 2024-T3 aluminium alloys, Prog. Org. Coat. (2009), doi:10.1016/j.porgcoat.2009.09.004